Simultaneous observations of magnetotail reconnection and bright X-ray aurora on 2 October 2002

A. L. Borg,[1] N. Østgaard,[2] A. Pedersen,[1] M. Øieroset,[3] T. D. Phan,[3] G. Germany,[4] A. Aasnes,[5] W. Lewis,[6] J. Stadsnes,[2] E. A. Lucek,[7] H. Rème,[8] and C. Mouikis[9]

Received 15 June 2006; revised 16 November 2006; accepted 21 November 2006; published 13 June 2007.

[1] We present simultaneous Cluster and Polar X-ray and UVI observations on 2 October 2002, when Cluster observed a magnetic reconnection diffusion region at Xgse = −16.6 Re. At the same time a bright auroral feature appeared at the footpoint of the magnetic field line connecting the ionosphere and the diffusion region. However, we found that the electrons measured in the diffusion region by Cluster were not sufficiently accelerated by the reconnection process to produce the aurora X-ray fluxes measured by Polar. The DMSP F14 passed over the intense X-ray spot and showed that the X rays (and the fainter UV) were produced by electrons accelerated through a ∼30 kV potential drop. The coincidence in time and the fact that this inverted-V is very close to the open-closed field line boundary suggest that the inverted-V structure are produced by flow shears that could be related to the reconnection process.

Citation: Borg, A. L., et al. (2007), Simultaneous observations of magnetotail reconnection and bright X-ray aurora on 2 October 2002, *J. Geophys. Res.*, *112*, A06215, doi:10.1029/2006JA011913.

1. Introduction

[2] The process known as magnetic reconnection converts magnetic energy into particle energy, accelerating particles away from the reconnection X-line. Magnetic reconnection relies on a breakdown of the frozen-in condition of electrons and ions. In the collisionless reconnection model, both ions and electrons move with the magnetic field lines initially. Inside an ion scale diffusion region, the ions diffuse from the magnetic field, leading to a separation of ions and electrons. The electrons become decoupled from the magnetic field lines in a smaller area known as the electron diffusion region. The separation of ions and electrons inside the ion diffusion region produces a quadrupolar Hall current system [*Sonnerup*, 1979]. These currents in turn induce a quadrupolar Hall magnetic field. Hall magnetic fields have been observed both for dayside magnetopause reconnection [*Mozer et al.*, 2002; *Vaivads et al.*, 2004] and in the magnetotail [*Nagai et al.*, 2001; *Øieroset et al.*, 2001; *Runov et al.*, 2003; *Asano et al.*, 2004; *Wygant et al.*, 2005; *Borg et al.*, 2005].

[3] Energetic electrons (several 100 keV to 1 MeV) observed in the magnetotail have also been attributed to the reconnection process [*Terasawa and Nishida*, 1976; *Baker and Stone*, 1976; *Baker and Stone*, 1977]. Little is known about how and where the electrons are accelerated. *Øieroset et al.* [2002] reported an observation of 300 keV electrons inside the diffusion region itself, while *Imada et al.* [2005] found that the highest intensity of energetic electrons flux is found away from the center of the X-type neutral region.

[4] Auroral signatures have been observed for high-latitude lobe reconnection during solar wind conditions with high pressure and strong northward IMF components [*Milan et al.*, 2000; *Frey et al.*, 2002; *Fuselier et al.*, 2002; *Phan et al.*, 2003; *Østgaard et al.*, 2005]. Searches for such signatures in connection with tail reconnection have also been made [*Fillingim et al.*, 2000; *Ieda et al.*, 2001; *Nakamura et al.*, 2001].

[5] In this paper we present simultaneous observations by the Cluster and Polar satellites on 2 October 2002. The Cluster observations show clear evidence of reconnection in the near-Earth magnetotail at $(X, Y, Z)_{GSE} = [-16.6, 8.0, 1.3]$ R_E near 2120 UT. At the same time a bright auroral feature appeared at the Cluster magnetic field line footpoint. An auroral spot moving over the footpoint is seen by both the UVI and PIXIE cameras on Polar, with the X-ray aurora being by far the brightest. We investigate whether the

[1]Department of Physics, University of Oslo, Oslo, Norway.
[2]Department of Physics, University of Bergen, Bergen, Norway.
[3]Space Sciences Laboratory, University of California, Berkeley, California, USA.
[4]Center for Space Plasma and Astronomy Research, University of Alabama in Huntsville, Huntsville, Alabama, USA.
[5]Space and Atmospheric Sciences, Los Alamos National Laboratory, Los Alamos, New Mexico, USA.
[6]Space Science Department, Southwest Research Institute, San Antonio, Texas, USA.
[7]Space and Atmospheric Physics, Imperial College London, London, UK.
[8]Centre d'Etude Spatiale des Rayonnements, Toulouse, France.
[9]Space Science Center, University of New Hampshire, Durham, New Hampshire, USA.

0148-0227/07/2006JA011913

auroral feature is related to the reconnection process in the tail.

2. Observations

2.1. Cluster Observations

[6] The focus of this study is a flow reversal observed by the Cluster satellites on 2 October 2002 around 2120 UT. The reference Cluster satellite, spacecraft 3 (SC3), was located at $(X, Y, Z)_{GSE}$ = [−16.6,8.0,1.3] R_E and the internal distances within the Cluster tetrahedron were about 4000 km. Because of the large internal separation the spacecraft measurements differ.

[7] We use data obtained by the plasma experiment (CIS) [*Rème et al.*, 2001], the magnetic field experiment (FGM) [*Balogh et al.*, 2001], the plasma electron and current experiment (PEACE) [*Johnstone et al.*, 1997] and the imaging energetic particle spectrometer experiment (RAPID) [*Wilken et al.*, 2001]. The CIS experiment does not operate on SC2. CIS 4s and FGM 0.04s resolution data from 2119:00 UT to 2124:00 UT are presented in Figure 1. For the SC1 and SC4 plasma velocity components in Figure 1b–1d, the H^+ composition measurements of the CIS/CODIF sensor were used. For the SC3 plasma velocity the CIS/HIA sensor was used because the CIS/CODIF data was inaccurate. The density is derived from the spacecraft potential, calibrated against the ion experiment. All data are presented in GSM coordinates.

[8] During the selected time interval, SC1 observed two flow reversals in the X direction from earthward (positive V_x) to tailward at 2120:20 UT and back to earthward at 2122:00 UT. V_x increased from 100 km/s to 600 km/s during the time interval 2119:30–2120:00 UT, decreased and crossed the zero line at 2120:20 UT, stayed negative until 2122:00 UT and then stayed mostly positive, with positive values reaching up to 500 km/s. V_y of SC1 remained positive with values up to 500 km/s except for two short intervals of negative values at 2119:48–2120:05 UT and 2120:40–2121:00 UT. V_z started at 400 km/s at the beginning of the time interval, decreased and turned negative at 2120:15 UT, returned to positive values at 2120:58 UT, and then finally to negative at 2122:45 UT.

[9] SC4 observed only one significant V_x flow reversal, from tailward to earthward at 2121:30 UT. V_x of SC4 followed mostly the same pattern of positive-negative-positive as SC1 V_x but did not see the first positive increase. SC4 V_x went from positive to negative at 2120:08 UT and back to positive at 2121:30 UT.

[10] SC3 V_x values were very small until 2121:00 UT, when the spacecraft observed an earthward flow with values up to 300 km/s. The flow lasted until 2122:30 UT. There was no flow reversal observed, and SC3 B_x indicates that the spacecraft remained near the southern lobe during the entire reconnection event.

[11] B_z of SC1 went from positive to negative at 2120:20 UT, changed briefly back to positive in the periods 2120:43–2121:00 UT and 2121:35–2121:40 UT, and then finally turned positive, and remained so for the rest of the time interval, at 2121:55 UT. B_z of SC4 changed from negative to positive values between 2122:10 UT and 2122:40 UT, increased slowly to positive values at 2123:35 UT, and returned briefly to negative between 2123:45 UT and 2123:55 UT. The timing of the flow reversals at SC1 and SC4 indicates that an X-line followed by an O-line [e.g., *Eastwood et al.*, 2005] traveled past the spacecraft in the earthward direction. In the present study we focus on the first (2120 UT) flow reversal and the associated reconnection diffusion region. The O-line crossing will be the topic of a separate study.

2.2. Polar Observations

[12] Polar was launched into an orbit with its apogee of 8.7 R_E over the northern hemisphere, but due to its apsidal precession Polar had its apogee just below the equator at 4.23 R_E during the Cluster observations presented above. We present images taken by the Ultraviolet Imager (UVI) [*Torr et al.*, 1995] and the Polar Ionospheric X-ray Imaging Experiment (PIXIE) [*Imhof*, 1995] over the southern hemisphere. We also present emissions in the Lyman-Hopfield-Birge-long band from UVI, 160–180 nm. These prompt emissions are negligibly affected by O_2 absorption and serve as a good indicator of total particle energy flux, which is usually dominated by the electron energy flux in the range 0.1–∼25 keV. PIXIE measures X-rays between 3.5 and 11 keV, which are produced by all electrons with energies larger than 3.5 keV, but as the X-ray production efficiency increases with higher electron energies, most of these X rays are produced by electron energies above 10 keV. For more information on the two instruments we refer to *Østgaard et al.* [2001]. We should emphasize that the X rays seen by PIXIE are only due to electron precipitation, as protons due to their much larger mass do not produce any X-ray bremsstrahlung.

[13] Figures 2a–2h show Polar X-ray (top) and UV (bottom) images from 2116 UT to 2124 UT on 2 October 2002. Accumulation/exposure time is 1 min and 36 s for PIXIE and UVI, respectively. The Cluster footpoint is shown in the figures as a red circle. This footpoint was estimated using the Tsyganenko 96 model. Although mapping from the tail to the ionosphere is usually highly uncertain, we have reasons to believe that the estimated footpoint is not very far from the true footpoint. The fact that there is only one X-ray spot and that the DMSP particle data clearly show that the precipitation is close to the open-closed boundary give us some confidence in the footpoint estimation.

[14] In the X-ray image of the time interval 2118–2119 UT (Figure 2c), we see emissions appearing between 2200 and 0100 local time. In the following images the emissions develop into a very bright spot that moves westward (to the right in these images from the southern hemisphere). The spot was located between 1900 and 2200 local time in the last plot at 2123–2124 UT (Figure 2h). The Cluster footpoint stayed well inside the spot from 2119 UT to approximately 2122 UT (Figures 2d–2f). From the UVI images it may seem that the Cluster footpoint was outside the UV spot. However, the UVI field-of-view (FOV) did not cover the Cluster footpoint before 2121:30 UT (Figure 2f), and at that time the X-ray spot had also passed the Cluster footpoint. From this we can conclude that either there was a UV spot outside the UVI FOV when the spot developed and passed the Cluster footpoint from 2118 UT to 2122 UT (Figures 2c–2f) or the energetic precipitation seen by PIXIE has a different morphology than the softer precipitation seen

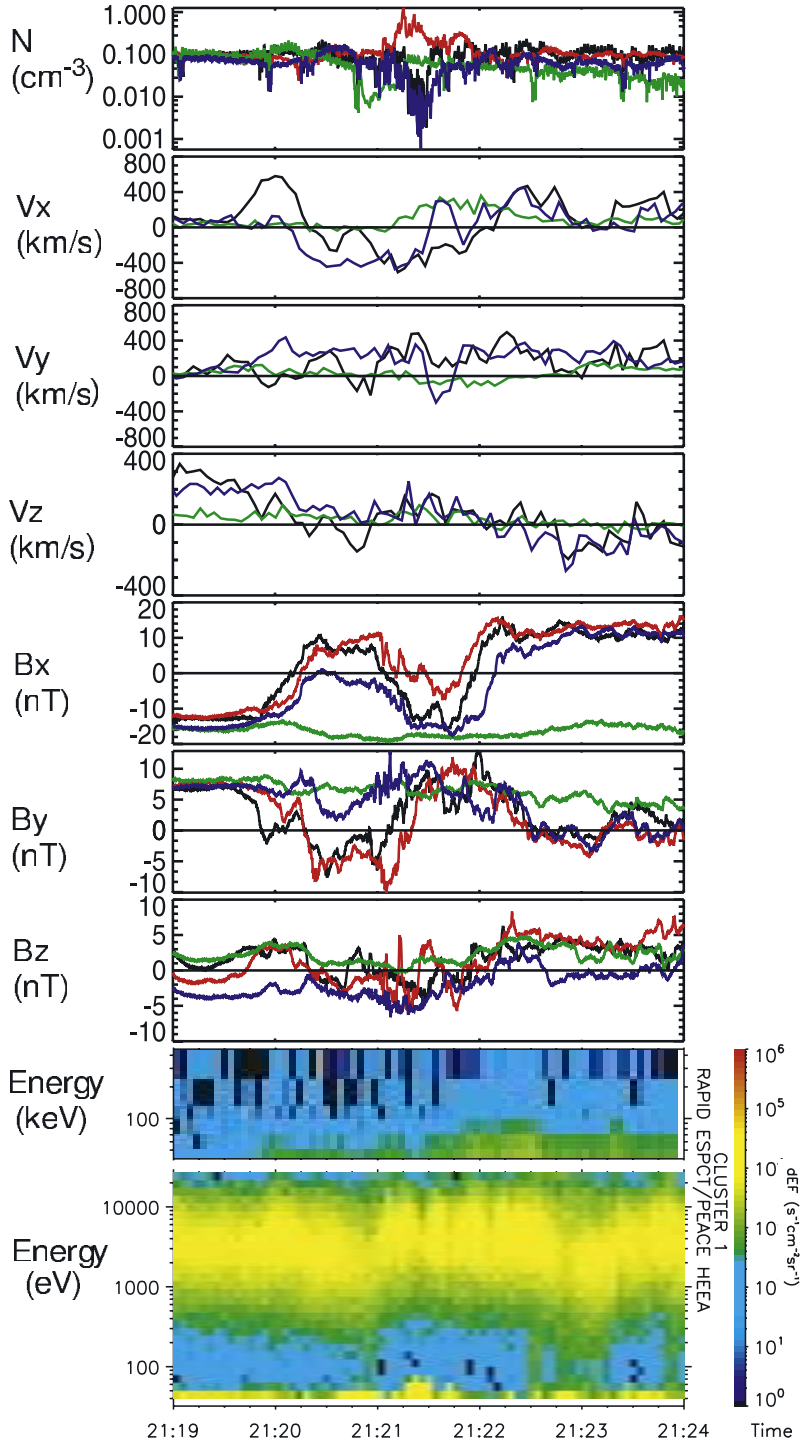

Figure 1. Cluster spacecraft observations for SC1 (black), SC2 (red), SC3 (green), and SC4 (blue) on 2 October 2002 for the time interval 2119:00–2124:00 UT. (a) Density converted from spacecraft potential; (b)–(d) SC1 and SC4: CODIF H^+ velocity (GSM), SC3: HIA velocity (no data from SC2); (e)–(g) magnetic field (GSM); (h)–(i) spin average spectrograms from SC1 PEACE and RAPID.

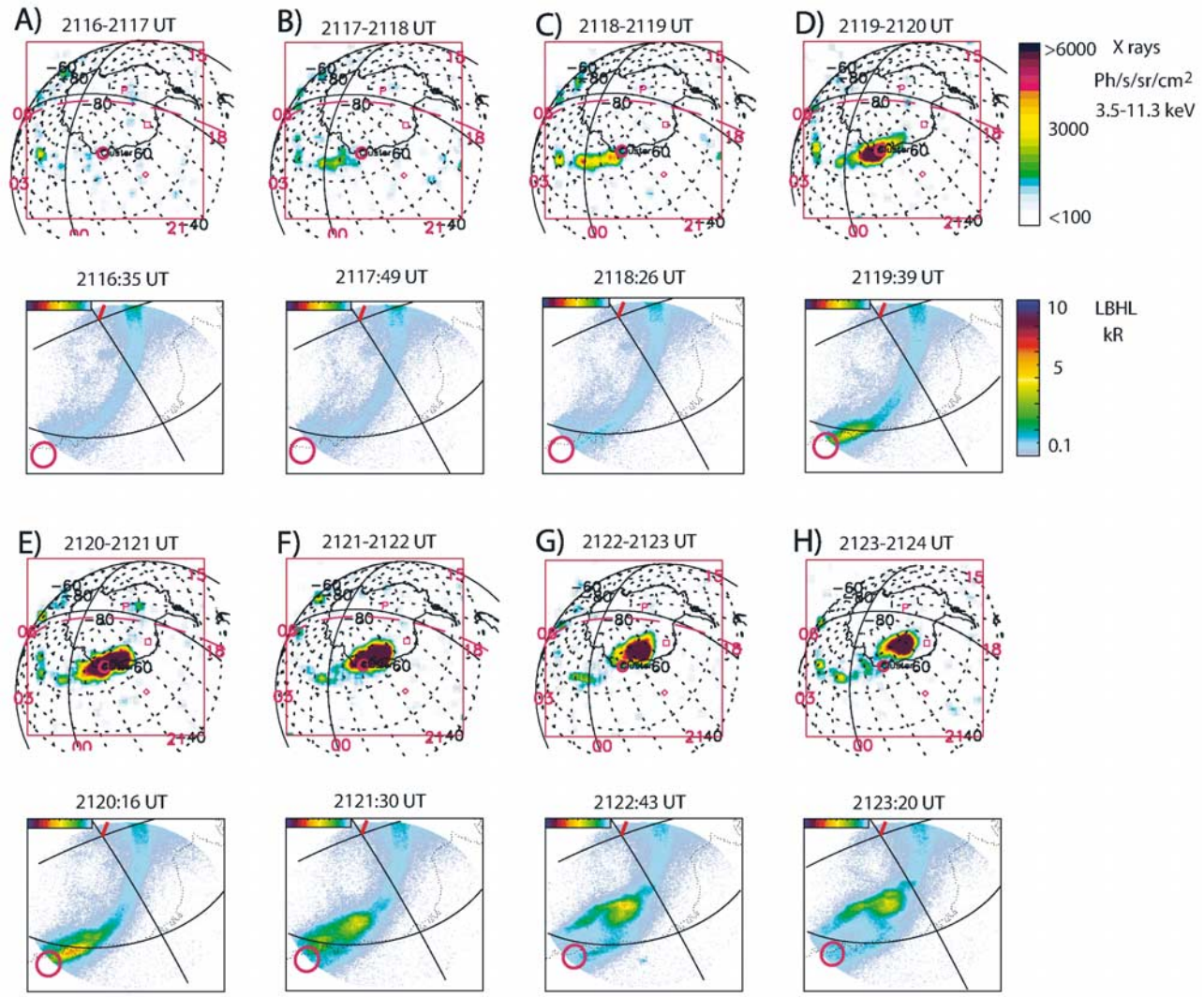

Figure 2. PIXIE X-ray and UVI images from 2116 UT to 2124 UT. PIXIE measures 3.5–11 keV X-rays and UVI measures UV emissions in the LBHL 160–180 nm band. Both PIXIE and UVI are mapped onto geographic coordinate system with the map showing Antarctica. Dashed lines in the PIXIE images show Corrected Geomagnetic grid while the solid lines in the UVI images show Geographic grid. Cluster magnetic field footpoint is marked with red circle.

by UVI. The latter possibility would be consistent with the findings of *Østgaard et al.* [1999].

3. Discussion

3.1. Flow Reversal in the Plasma Sheet

[15] Flow reversals were observed by SC1 and SC4, starting at 2119:30 UT for SC1 and at 2120:10 UT for SC4. V_x and B_z of SC1 and SC4 in Figures 1b and 1g change polarity at approximately the same time, suggesting that the center of the diffusion region moved over SC1 in the earthward direction at 2120:20 UT.

[16] Looking at the density, we see in Figure 1a that both the SC1 and the SC4 density dropped from about 0.10 cm^{-3} down to approximately 0.005 cm^{-3}, which is close to lobe density values, at around 2121:30 UT. This suggests that SC1 stayed inside the plasma sheet during the reversals but came close to a separatrix between reversals. The SC4 density drop occurred around the time of the SC4 V_x flow reversal suggesting that this spacecraft moved close to the separatrix at this time. Density minima have been predicted to occur near the separatrices [*Shay et al.*, 2001], where large electric fields have also been reported [*Borg et al.*, 2005]. Also, noting that V_x went through a gradual transition at the first flow reversal, we conclude that SC1 did not pass through the inflow region, but remained inside the reconnection layer.

3.2. Hall Magnetic Field

[17] The collisionless reconnection model predicts a quadrupole magnetic field in the diffusion region in the out-of-plane direction [*Sonnerup*, 1979]. SC1 observed both earthward and tailward flow in the time interval 2119:00–2124:00 UT and entered both the northern and the southern hemispheres. The satellites could therefore have detected several branches of the Hall magnetic field. However, the

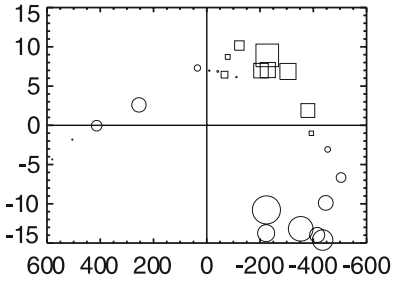

Figure 3. Hall magnetic field: B_i (close to B_x) versus V_i (close to V_x) with B_j (close to B_y) represented as circles (positive B_j) and squares (negative B_j) for SC1 (2120:00–2121:40 UT). The size of the symbols is relative to the magnitude of B_j. B_i and B_j plotted here have been obtained by using minimum variance analysis [*Sonnerup and Cahill*, 1967]. The maximum, intermediate, and minimum variance directions are i = (0.96x, −0.25y, 0.11z), j = (0.19x, 0.90y, 0.28z), and k = (−0.19, −0.35, 0.92). The eigenvalue ratio $e_j/e_k = 20$ is good and indicates that the minimum variance direction is well determined.

time intervals chosen for the Hall magnetic field investigation must satisfy the following criteria: The spacecraft (1) must observe a reconnection jet (large positive or negative V_x) and (2) must be located inside the plasma sheet. The SC1 data satisfied these criteria in the time interval 2120:00–2121:40 UT.

[18] We have performed the Hall magnetic field analysis in the current sheet normal coordinate system determined from minimum variance analysis of the magnetic field [*Sonnerup and Cahill*, 1967]. In this coordinate system, i, j, and k are slightly rotated from the GSM x, y, and z directions; see caption of Figure 3 for more details. In Figure 3 the out-of-plane (B_j) magnetic field for SC1 is plotted. The plot shows V_i versus B_i with the B_j variable represented by squares and circles. The squares indicate negative B_j values, while the circles indicate positive B_j values. The size of each symbol is proportional to the magnitude of B_j.

[19] The out of plane (Hall) magnetic field is a quadrupole field induced by currents originating in the diffusion region. When the Hall magnetic field polarity is added to a V_i versus B_i plot, we expect negative values when $V_i < 0$, $B_i > 0$ and $V_i > 0$, $B_i < 0$, and positive values for the conditions $V_i < 0$, $B_i < 0$ and $V_i > 0$, $B_i > 0$.

[20] We see that SC1 observed three branches of a clear Hall magnetic field quadrupole configuration, although there are a few, small value B_j deviations. SC1 observed negative B_j values when $V_i < 0$, $B_i > 0$ and positive B_j values were observed for the conditions $V_i < 0$, $B_x < 0$ and $V_x > 0$, $B_x > 0$, as expected for the quadrupole Hall magnetic fields.

3.3. Cluster and POLAR

[21] We note that the bright X-ray auroral spot measured by Polar covered the Cluster footpoint at the time when Cluster observed a reconnection diffusion region. This suggests that the precipitation seen by Polar might be caused by energetic electrons accelerated in the diffusion region. As mentioned earlier, the observed X rays are only due to electron precipitation as protons do not produce any X-ray bremsstrahlung.

[22] The thick lines in Figure 4a show the averaged X-ray intensity within a circle with a radius of 300 km around the Cluster footpoint. This corresponds to the spatial resolution of the PIXIE camera. The X-ray intensity reached a maximum around 2121 UT. Comparing with Figure 1, we see that the footpoint maximum coincided with the Cluster 1 and 4 observations of a tailward flow of ions (V_x negative) corresponding to a diffusion region having moved earthward.

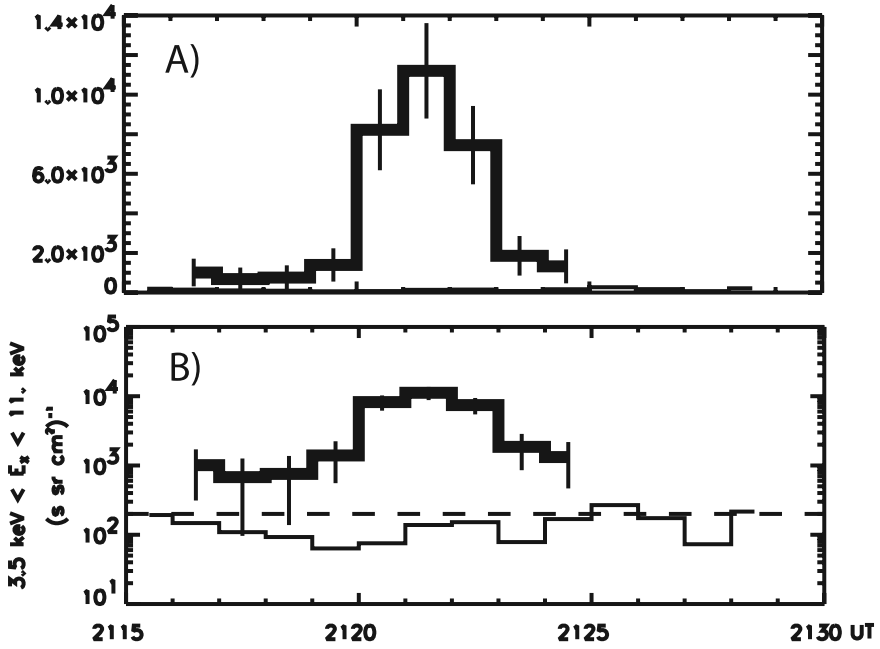

Figure 4. Measured and estimated X-rays. (a) Linear scale. Thick line is the measured X-ray flux from PIXIE. Thin line is the estimated X-ray production by the electrons measured by RAPID and PEACE. (b) Logarithmic scale. Dashed line indicates the noise level in the PIXIE measurements.

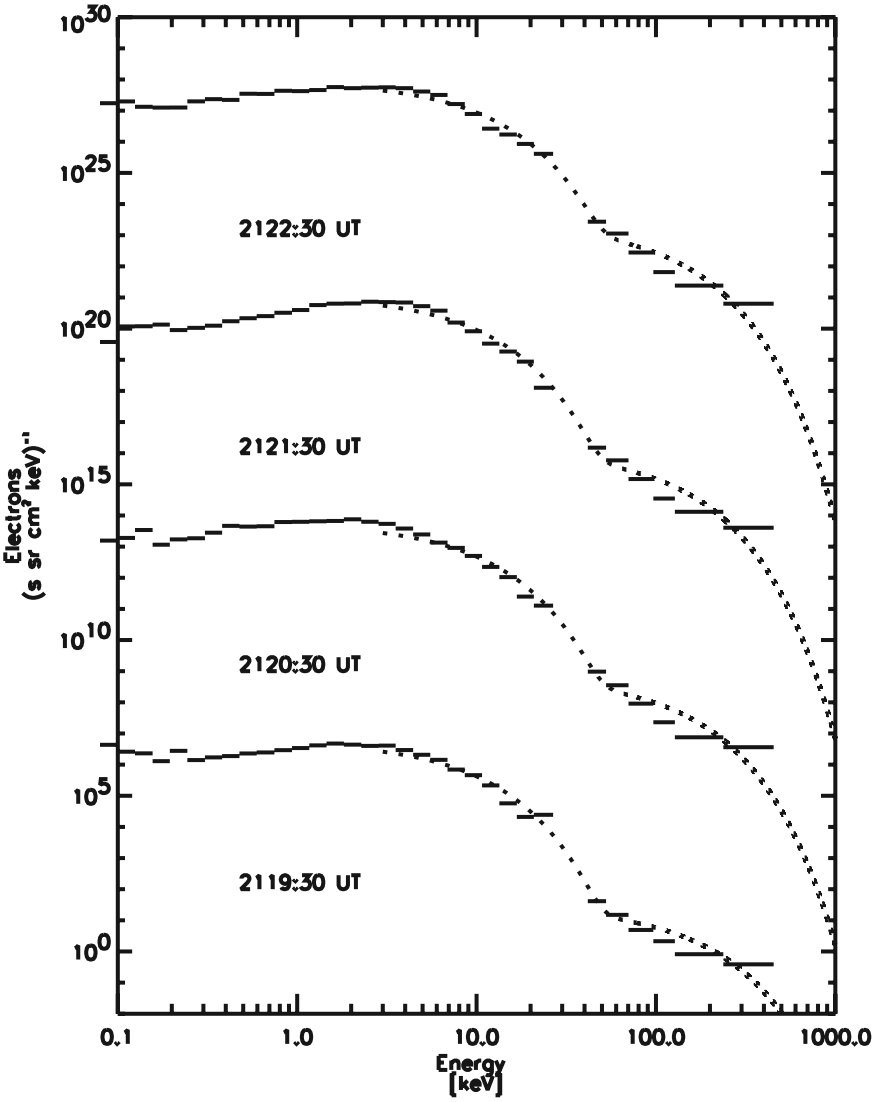

Figure 5. Electron spectra from RAPID and PEACE. One-minute average spectra from 0 to 7.5 degree pitch angle from PEACE and spin averaged from RAPID. The spectra are shifted by 10^7.

[23] Using data from Cluster's PEACE and RAPID instruments in the energy range 3.5–453 keV, we can estimate the X-rays that would be produced in the ionosphere by the electron distribution measured in the magnetotail. This allows us to test the hypothesis that the electrons responsible for the auroral signatures were accelerated by the reconnection process observed by Cluster. We have used the PEACE measurements (32 eV to 26.7 keV) within ±7.5 degree pitch angle of the loss cone. The RAPID measurements (41.7–453 keV) were only available as spin averaged data. As the fluxes within the ±7.5 degree pitch angle from PEACE were only slightly larger than the spin averaged fluxes, we think that the electron distribution was rather isotropic, giving us confidence in using the spin-averaged data from RAPID. However, as the loss cone at 18 Re is only a fraction of a degree, a resolution of 7.5 degree is not good enough to resolve any anisotropy in the loss cone. This is of course a source of error for our estimates.

[24] To make an estimate of the X-ray production, we proceeded as follows: First, we made a double exponential fit to the measured electron spectra (see example in Figure 5), then we used a look-up table of angular-dependent X-ray spectra generated on the basis of the "general electron-photon transport code" of *Lorence* [1992] for a wide range of exponential spectra and atmospheric escaping angles. This code takes into account the scattering of electrons, production of secondary electrons, angular dependent X-ray production, photoelectric absorption of X rays, and Compton scattering of X rays. Information about the exact viewing angle of PIXIE were used to get estimates of X rays with the correct escaping angle. The code and procedure described here has been shown to estimate expected X-ray fluxes [*Østgaard et al.*, 2000] as well as electron spectra from X-ray fluxes [*Østgaard et al.*, 2001] for electron energies >3 keV. For the estimates presented in this paper, we have made two assumptions. (1) The electron distribution is isotropic within the ±7.5 degree pitch angle interval. (2) If reconnection alone is responsible for the acceleration, there are no other adiabatic accelaration processes from the tail to the ionosphere. This means that most of the X-rays are produced by electrons well below

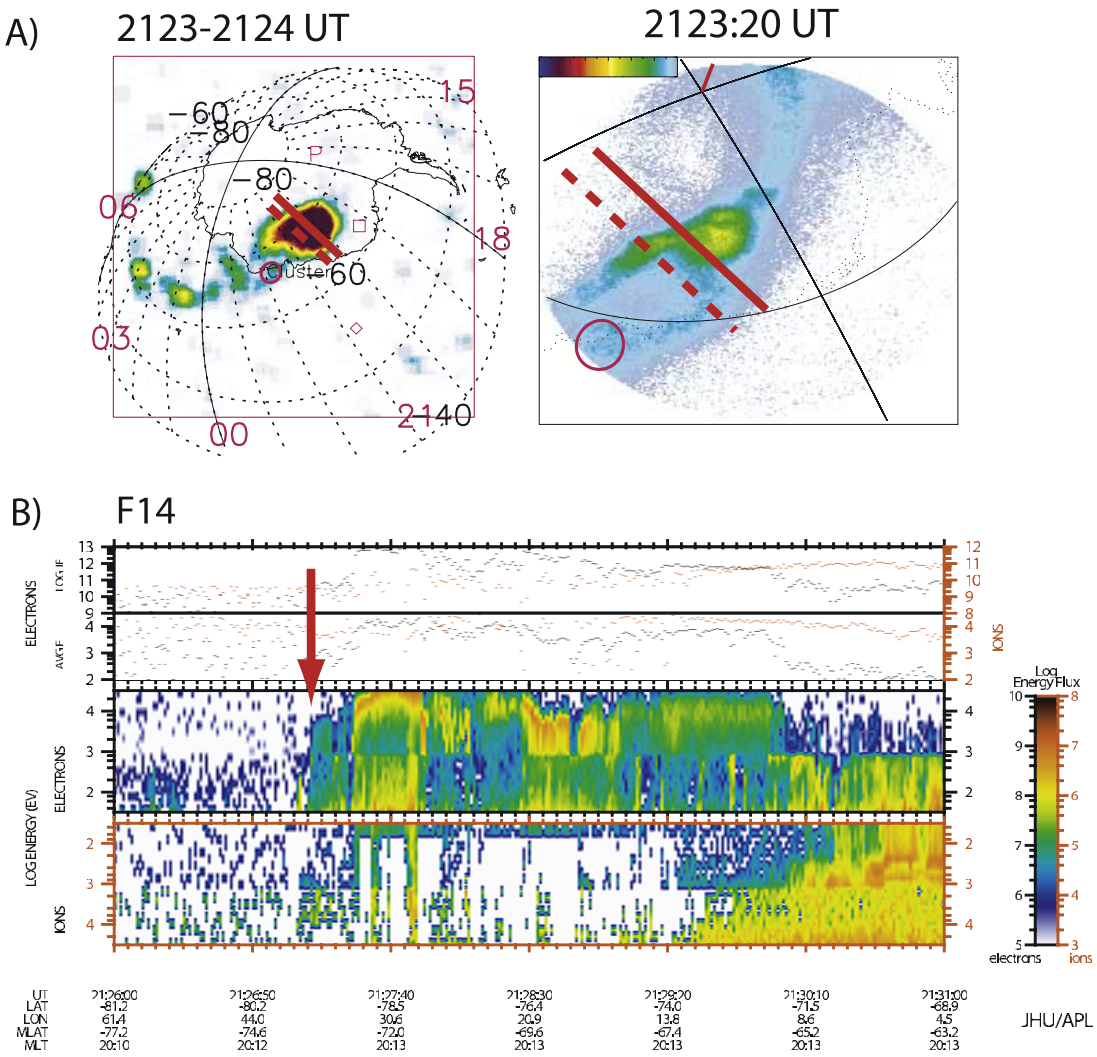

Figure 6. (a) PIXIE (left) and UVI (right) images ~4 min earlier than DMSP passed through the inverted-V structure. Red lines show DMSP trajectory and dashed red line if we assume that the spot continued to move duskward from 2123 UT to 2127 UT. The grids are explained in Figure 2. (b) The DMSP F14 pass through the intense auroral spot. Red arrow indicates the open/closed field line boundary.

50 keV, while the contributions from electrons above ~50 keV is negligible. The integrated X-ray production from electrons above 50 keV is two orders of magnitude lower than from the electrons below 50 keV. It may be argued that a power-law fit should be used instead of an exponential fit, but for the very low fluxes of electrons >50 keV, this would not make any difference.

[25] In Figure 4b we present both the directly measured time profile by PIXIE (thick line) and the estimated X-ray fluxes produced by the Cluster measurements (thin line). Compared to the measured X-ray fluxes, the estimated X-ray fluxes are one or two orders of magnitude too low and they have a different temporal behavior. The dashed line indicates the noise level in the PIXIE measurements. From this comparison it is clear that the electrons as measured by Cluster are not responsible for the auroral signatures seen by PIXIE. Earlier studies [*Fillingim et al.*, 2002] have also suggested that the plasma sheet energy flux can not account for the energy flux in the ionosphere during periods of large auroral activity. *Wygant et al.* [2000] and *Keiling et al.* [2002] suggest an acceleration of electrons from the magnetotail above the auroral acceleration region, primarily by Alfvèn waves.

[26] We therefore have the following case: (1) Cluster observations clearly demonstrates that Cluster SC1 passed through the reconnection diffusion region. (2) At no time during this pass does Cluster measure electron fluxes that can produce any PIXIE observable X-rays in the ionosphere. (3) PIXIE, on the other hand, does see a bright spot that coincided in time with Cluster observing a reconnection diffusion region. This auroral spot would map to a wide region in the plasma sheet, which is very likely to include the position of the Cluster spacecraft. We have two candidate explanations for these observations:

[27] 1. Owing to errors in the field line mapping the Cluster footpoint may not be inside the X-ray spot. Although this explanation is not very likely (see point 3 above about the

wide mapping region), it implies that there must be other mechanisms than the reconnection process seen by Cluster accelerating the particles.

[28] 2. This leads us to the more likely explanation that the particles are accelerated somewhere along the field lines from Cluster at 17 R_E to the ionosphere.

[29] The evidence for the second scenario is the measurements by a fortuitous overpass by DMSP F14. As shown in Figure 6, this low-altitude satellite passed through the intense auroral spot only ~4 min after the last Polar image (see Figure 6a). The dashed line indicates the DMSP pass through the X-ray spot given that the X-ray spot continued to move duskward from 2123 UT to 2127 UT with the same speed as it did prior to 2123 UT. From Figure 6b it is clear that DMSP passed through an inverted-V structure with a relatively large peak value of >30 keV.

[30] The inverted-V structure is seen by DMSP between 70.5 and 72.5 degree MLAT with the poleward edge less than 100 km (0.9 degree latitude) from the open-closed boundary, as determined from the DMSP particle data. Although the Cluster footpoint at this time is ~3 degrees equatorward of the inverted-V, we know that the inverted-V structure passed the estimated footpoint of Cluster between 2119 UT and 2121 UT (Figure 2d and 2e). This coincides exactly in time with the flow reversal observed by Cluster. The very large potential drop resulting in an electron distribution with high fluxes above 20 keV and very few electrons below 20 keV explains thoroughly why the X-ray spot is intense, while the UV emissions are weak (<1 kR). This is consistent with the sensitivity of the two cameras as we described in section 2.2. We have calculated the expected X-ray and UV production from three spectra measured by DMSP as the spacecraft passed through the inverted-V structure. Calculation of X-ray production based on thick-target bremsstrahlung theory [*Vij et al.*, 1975] gives 1.6–4.0 10^4 $(s \cdot sr \cdot cm^2)^{-1}$ X-ray photons. A calculation of UV emission in the LBHL band gives 1.4–3.3 kR. Given that we do not know if the DMSP footpoint intersects exactly with the footpoint of Cluster, these estimates are very close to $\sim 10^4$ $(s \cdot sr \cdot cm^2)^{-1}$ (Figure 4) and ~1 kR that PIXIE and UV measured (Figure 2), respectively.

[31] A likely cause for such an inverted-V structure is strong convecting flow shears that produce large converging electric field and field-aligned potential drops [*Gurnett and Frank*, 1973; *Reiff et al.*, 1978]. The coincidence in time and the fact that this inverted-V is very close to the open-closed field line boundary suggest that the potential drop is not just a coincidence but rather related to the reconnection process.

4. Conclusion

[32] In this paper we have reported a rare coincidence of simultaneously observing the reconnection process in the Near-Earth plasma sheet and a bright auroral X-ray spot at the footpoint of the field line connecting the ionosphere and the diffusion region.

[33] 1. Timing analysis shows that the two flow reversals observed by SC1 at about 2120 UT and 2122 UT are due to the earthward motion of an X-line followed by an O-line. The first flow reversal (seen in SC1) is gradual with a matching Bz reversal and the spacecraft remained inside the plasma sheet, consistent with a diffusion region crossing. Three branches of the Hall magnetic field was observed in this diffusion region encounter.

[34] 2. A bright X-ray spot was observed by Polar PIXIE from 2119 UT to 2122 UT at the footpoint of the Cluster magnetic field line, coinciding with the Cluster observation of the reconnection diffusion region in the tail.

[35] 3. Contrary to what one would expect from the correspondence of the Cluster reconnection region to the PIXIE X-ray spot, we found no direct relation between the reconnection process and the bright spot. Using particle measurements from the RAPID and PEACE experiments on Cluster to estimate the X-ray production, we have demonstrated that the reconnection process did not accelerate particles to energies that could have produced the observed X rays.

[36] 4. A DMSP F14 pass through the intense X-ray spot shows clearly that the X-rays (and the fainter UV) were produced by electrons accelerated by a ~30 kV potential drop. The coincidence in time and the fact that this inverted-V is very close to the open-closed boundary may suggest that the inverted-V structure is related to the reconnection process.

[37] **Acknowledgments.** This work has been supported by the Research Council of Norway. The work done at UC Berkeley was supported by NASA grant NNG05GE30G. We thank both the referees for their constructive comments.

[38] Wolfgang Baumjohann thanks Shinsuke Imada and Victor Sergeev for their assistance in evaluating this paper.

References

Asano, Y., T. Mukai, M. Hoshino, Y. Saito, H. Hayakawa, and T. Nagai (2004), Current sheet structure around the near-Earth neutral line observed by Geotail, *J. Geophys. Res.*, *109*, A02212, doi:10.1029/2003JA010114.

Baker, D. N., and E. C. Stone (1976), Energetic electron anisotropies in the magnetotail: Identification of open and closed field lines, *Geophys. Res. Lett.*, *3*, 557–560.

Baker, D. N., and E. C. Stone (1977), Observations of energetic electrons E no less than about 200 keV in the earth's magnetotail: Plasma sheet and fireball observations, *J. Geophys. Res.*, *82*, 1532–1546.

Balogh, A., et al. (2001), The Cluster Magnetic Field Investigation: overview of in-flight performance and initial results, *Ann. Geophys.*, *19*, 1207–1217.

Borg, A. L., et al. (2005), Cluster encounter of a magnetic reconnection diffusion region in the near-Earth magnetotail on September 19, 2003, *Geophys. Res. Lett.*, *32*, L19105, doi:10.1029/2005GL023794.

Eastwood, J. P., D. G. Sibeck, J. A. Slavin, M. L. Goldstein, B. Lavraud, M. Sitnov, S. Imber, A. Balogh, E. A. Lucek, and I. Dandouras (2005), Observations of multiple X-line structure in the Earth's magnetotail current sheet: A Cluster case study, *Geophys. Res. Lett.*, *32*, L11105, doi:10.1029/2005GL022509.

Fillingim, M. O., G. K. Parks, L. J. Chen, M. Brittnacher, G. A. Germany, J. F. Spann, D. Larson, and R. P. Lin (2000), Coincident POLAR/UVI and WIND observations of pseudobreakups, *Geophys. Res. Lett.*, *27*, 1379–1382.

Fillingim, M. O., G. K. Parks, R. P. Lin, and D. Chua (2002), Comparison of plasma sheet and auroral electron energy fluxes during substorms, *Proc. Int. Conf. Substorms*, *6*, 382.

Frey, H. U., et al. (2002), Proton aurora in the cusp, *J. Geophys. Res.*, *107*(A7), 1091, doi:10.1029/2001JA900161.

Fuselier, S. A., et al. (2002), Cusp aurora dependence on interplanetary and lobe magnetic field B_z, *J. Geophys. Res.*, *107*(A7), 1111, doi:10.1029/2001JA900165.

Gurnett, D. A., and L. A. Frank (1973), Observed relationships between electric fields and auroral particle precipitation, *J. Geophys. Res.*, *78*, 145.

Ieda, A., D. H. Fairfield, T. Mukai, Y. Saito, S. Kokubun, K. Liou, C.-I. Meng, G. K. Parks, and M. J. Brittnacher (2001), Plasmoid ejection and auroral brightenings, *J. Geophys. Res.*, *106*, 3845–3858.

Imada, S., M. Hoshino, and T. Mukai (2005), Average profiles of energetic and thermal electrons in the magnetotail reconnection regions, *Geophys. Res. Lett.*, *32*, L09101, doi:10.1029/2005GL022594.

Imhof, W. L. (1995), The Polar ionospheric X-ray-imaging experiment (PIXIE), *Space Sci. Rev.*, *71*, 385–408.

Johnstone, A. D., et al. (1997), PEACE: A plasma electron and current experiment, *Space Sci. Rev.*, *79*, 351–398, doi:10.1023/A:1004938001388.

Keiling, A., J. R. Wygant, C. Cattell, W. Peria, G. Parks, M. Temerin, F. S. Mozer, C. T. Russell, and C. A. Kletzing (2002), Correlation of Alfvn wave Poynting flux in the plasma sheet at 4-7 RE with ionospheric electron energy flux, *J. Geophys. Res.*, *107*(A7), 1132, doi:10.1029/2001JA900140.

Lorence, L. J. (1992), CEPXS ONELD version 2.0: A discrete ordinates code package for general one-dimensional coupled electron-photon transport, *IEEE Trans. on Nucl. Sci.*, *39*, 1031–1034.

Milan, S. E., M. Lester, S. W. H. Cowley, and M. Brittnacher (2000), Dayside convection and auroral morphology during an interval of northward interplanetary magnetic field, *Ann. Geophys.*, *18*, 436–444.

Mozer, F. S., S. D. Bale, and T. D. Phan (2002), Evidence of diffusion regions at a subsolar magnetopause crossing, *Phys. Rev. Lett.*, *89*(1), 015002, doi:10.1103/PhysRevLett.89.015002.

Nagai, T., et al. (2001), Geotail observations of the Hall current system: Evidence of magnetic reconnection in the magnetotail, *J. Geophys. Res.*, *106*, 25,929–25,950.

Nakamura, R., W. Baumjohann, M. Brittnacher, V. A. Sergeev, M. Kubyshkina, T. Mukai, and K. Liou (2001), Flow bursts and auroral activations: Onset timing and foot point location, *J. Geophys. Res.*, *106*, 10,777–10,790.

Øieroset, M., et al. (2001), In situ detection of collisionless reconnection in the Earth's magnetotail, *Nature*, *412*, 414–417.

Øieroset, M., R. P. Lin, T. D. Phan, D. E. Larson, and S. D. Bale (2002), Evidence for electron acceleration up to 300 keV in the magnetic reconnection diffusion region of Earth's magnetotail, *Phys. Rev. Lett.*, *89*(19), 195001.

Østgaard, N. (1999), Global scale electron precipitation features seen in UV and X-rays during substorms, *J. Geophys. Res.*, *104*, 10,191–10,204.

Østgaard, N., et al. (2000), Cause of the localized maximum of X-ray emission in the morning sector: A comparison with electron measurements, *J. Geophys. Res.*, *105*, 20,869–20,885.

Østgaard, N., et al. (2001), Auroral electron distributions derived from combined UV and X-ray emissions, *J. Geophys. Res.*, *106*, 26,081–26,089.

Østgaard, N., S. B. Mende, H. U. Frey, and J. B. Sigwarth (2005), Simultaneous imaging of the reconnection spot in the conjugate hemispheres during northward IMF, *Geophys. Res. Lett.*, *32*(21), L21104, doi:10.1029/2005GL024491.

Phan, T., et al. (2003), Simultaneous Cluster and IMAGE observations of cusp reconnection and auroral proton spot for northward IMF, *Geophys. Res. Lett.*, *30*(10), 1509, doi:10.1029/2003GL016885.

Reiff, P. H., J. L. Burch, and R. A. Heelis (1978), Dayside auroral arcs and convection, *Geophys. Res. Lett.*, *5*, 391.

Rème, H., et al. (2001), First multispacecraft ion measurements in and near the Earth's magnetosphere with the identical Cluster ion spectrometry (CIS) experiment, *Ann. Geophys.*, *19*, 1303–1354.

Runov, A., et al. (2003), Current sheet structure near magnetic X-line observed by Cluster, *Geophys. Res. Lett.*, *30*(11), 1579, doi:10.1029/2002GL016730.

Shay, M. A., et al. (2001), Alfvénic collisionless magnetic reconnection and the Hall term, *J. Geophys. Res.*, *106*, 3759–3772.

Sonnerup, B. U. Ö. (1979), *Solar System Plasma Physics*, vol. III, edited by L. T. Lanzerotti, C. F. Kennel, and E. N. Parker. pp. 45-108, Elsevier, New York.

Sonnerup, B. U. Ö., and L. J. Cahill (1967), Magnetopause structure and attitude from Explorer 12 observations, *J. Geophys. Res.*, *72*, 171.

Terasawa, T., and A. Nishida (1976), Simultaneous observations of relativistic electron bursts and neutral-line signatures in the magnetotail, *Planet. Space Sci.*, *24*, 855.

Torr, M. R., et al. (1995), A far-ultraviolet imager for the international solar-terrestrial physics mission, *Space Sci. Rev.*, *71*, 329–383.

Vaivads, A., et al. (2004), Structure of the magnetic reconnection diffusion region from four-spacecraft observations, *Phys. Rev. Lett.*, *93*(10), 105001, doi:10.1103/PhysRevLett.93.105001.

Vij, K. K., D. Venkatesan, W. R. Sheldon, J. W. Kern, J. R. Benbrook, and B. A. Whalen (1975), Simultaneous investigation of parent electrons and Bremsstrahlung X-Rays by rocket-borne detectors, *J. Geophys. Res.*, *80*, 2869–2875.

Wilken, B., et al. (2001), First results from the RAPID imaging energetic particle spectrometer on board Cluster, *Ann. Geophys.*, *19*, 1355–1366.

Wygant, J. R., et al. (2000), Polar spacecraft based comparisons of intense electric fields and Poynting flux near and within the plasma sheet-tail lobe boundary to UVI images: An energy source for the aurora, *J. Geophys. Res.*, *105*, 18,675–18,692.

Wygant, J. R., et al. (2005), Cluster observations of an intense normal component of the electric field at a thin reconnecting current sheet in the tail and its role in the shock-like acceleration of the ion fluid into the separatrix region, *J. Geophys. Res.*, *110*, A09206, doi:10.1029/2004JA010708.

A. Aasnes, ISR 1, Space and Atmospheric Sciences, Los Alamos National Laboratory, Los Alamos, NM, USA.

A. L. Borg and A. Pedersen, Department of Physics, University of Oslo, Oslo N-0316, Norway. (a.l.borg@fys.uio.no)

G. Germany, S131 Technology Hall, University of Alabama in Huntsville, Huntsville, AL 35899, USA.

W. Lewis, Space Science Department, Space Research and Engineering Division, Southwest Research Institute, San Antonio, TX 78228-0510, USA.

E. A. Lucek, Space and Atmospheric Physics, Imperial College London, London SW7 2BZ, UK.

C. Mouikis, Space Science Center, University of New Hampshire, Durham, NH 03824-3535, USA.

M. Øieroset and T. D. Phan, Space Sciences Laboratory, University of California, Berkeley, Berkeley, CA 94720, USA.

N. Østgaard and J. Stadsnes, Department of Physics, University of Bergen, Allegaten 55, N-5007 Bergen, Norway.

H. Rème, Centre d'Etude Spatiale des Rayonnements, F-31028 Toulouse, France.